

Mode structure and orbital angular momentum of spatiotemporal optical vortex (STOV) pulses

S.W. Hancock, S. Zahedpour, and H.M. Milchberg

*Institute for Research in Electronics and Applied Physics
University of Maryland, College Park, MD 20742*

Abstract

We identify a class of modal solutions for spatio-temporal optical vortex (STOV) electromagnetic pulses propagating in dispersive media. We find that STOVs can carry half-integral units of intrinsic orbital angular momentum (OAM) in vacuum, with OAM orthogonal to propagation. Our results also suggest that STOVs propagating in dispersive media are accompanied by half-integral units of OAM associated with a polariton-like quasiparticle. Consideration of spatiotemporal phase circulation around a STOV singularity suggests that single-valuedness of states under such rotations is not a constraint for electromagnetic fields.

Several years ago, we reported on the first experimental measurement of spatiotemporal optical vortices (STOVs), which were found to emerge from the self-focusing collapse arrest and filamentation of femtosecond optical pulses in air [1]. STOVs appear to underlie all self-focusing collapse scenarios, including relativistic self-focusing in plasmas and filamentation in transparent solids. More recently, we demonstrated generation of STOV-carrying pulses using a $4f$ pulse shaper and studied their free space propagation from near field to far field, capturing their evolving spatio-temporal amplitude and phase [2], with this work later verified in experiments observing STOVs only in the far field [3]. Our recent experiments demonstrating STOV OAM conservation in second harmonic generation strongly suggests that STOV OAM applies at the single photon level [4-6]. With that result, it appears that STOV-carrying pulses may have significant potential for science and technology.

The subject of spatial optical vortices garnered renewed interest when Allen *et al.* [7] demonstrated a fundamental connection between intrinsic spatial OAM and Laguerre-Gaussian modes of integer topological charge l : such beams carried OAM of $l\hbar$ per photon. The beams considered by Allen are monochromatic, with the vortex axis, angular momentum, and linear momentum all aligned. Closer to our situation, Sukhorukov and Yangirova [8] have suggested the possibility of measuring spatiotemporal vortices and Bliokh and Nori [9] have considered dispersionless vortices in the spatiotemporal domain.

In this paper, we present a theoretical description of STOV-carrying pulses in both vacuum and in material media, with emphasis on their mode structure and spatiotemporal orbital angular momentum. STOVs take on additional character in dispersive media, where their phase winding drives dispersive evolution. Our results show that STOVs in vacuum can carry half-integral OAM, and that in dispersive media they support quasiparticles with half integral OAM shared with the light. Recent theoretical work by Bliokh [10] has also considered spatiotemporal vortex pulses, but without a full modal analysis in dispersive media that reveals the true nature of STOV OAM.

We start by looking for STOV-supporting modal solutions of the paraxial wave equation. To account for possible medium dispersion, we use the Fourier transformed wave equation for a uniform isotropic medium with dielectric function $\varepsilon(\omega)$ and wavenumber given by $k^2(\omega) = \omega^2 \varepsilon(\omega)/c^2$,

$$\left(\nabla_{\perp}^2 + \frac{\partial^2}{\partial z^2} + k^2(\omega) \right) \tilde{\mathbf{E}}(\mathbf{r}_{\perp}, z, \omega) = 0, \quad (1)$$

where $\tilde{\mathbf{E}}$ is the $t \rightarrow \omega$ Fourier-transformed field, pulse propagation is along $\hat{\mathbf{z}}$, \mathbf{r}_{\perp} represents transverse coordinates orthogonal to $\hat{\mathbf{z}}$, and ∇_{\perp}^2 is the corresponding transverse Laplacian. We assume $\tilde{\mathbf{E}}(\mathbf{r}_{\perp}, z, \omega) = \tilde{\mathbf{A}}(\mathbf{r}_{\perp}, z, \omega - \omega_0) e^{ik_0 z}$, where $\tilde{\mathbf{A}}$ is a slowly varying envelope and $k_0 = k(\omega_0)$ is the wavenumber at the central frequency. This yields $(\nabla_{\perp}^2 + 2ik_0 \partial/\partial z) \tilde{\mathbf{A}} + (k^2(\omega) - k_0^2) \tilde{\mathbf{A}} = 0$ for $k_0 |\partial \tilde{\mathbf{A}}/\partial z| \gg |\partial^2 \tilde{\mathbf{A}}/\partial z^2|$. Using $k^2(\omega) - k_0^2 \approx 2k_0(k(\omega) - k_0)$ and expanding $k(\omega) = k_0 + k'_0(\omega - \omega_0) + k''_0(\omega - \omega_0)^2/2 + \dots$ gives $2ik_0 \partial \tilde{\mathbf{A}}/\partial z = -\nabla_{\perp}^2 \tilde{\mathbf{A}} - 2k_0(k'_0 \omega + k''_0 \omega^2 + \dots) \tilde{\mathbf{A}}$, where $k'_0 = (\partial k/\partial \omega)_0 = v_g^{-1}$ is the inverse group velocity at ω_0 , and $k''_0 = (\partial^2 k/\partial \omega^2)_0 = (\partial v_g^{-1}/\partial \omega)_0$ is the group velocity dispersion (GVD). Assuming that the pulse bandwidth is not too large ($\Delta\omega/\omega_0 \ll 1$), keeping terms in the $k(\omega)$ expansion to second order is an excellent approximation. This gives, after transforming back to the time domain, $2ik_0 \partial \mathbf{A}/\partial z = -(\nabla_{\perp}^2 + 2ik_0 k'_0 \partial/\partial t - k_0 k''_0 \partial^2/\partial t^2) \mathbf{A}$ where $\mathbf{A} = \mathbf{A}(\mathbf{r}_{\perp}, z, t)$. Finally, we make the substitutions $\xi = v_g t - z$ and $\beta_2 = v_g^2 k_0 k''_0$ to give

$$2ik_0 \frac{\partial}{\partial z} \mathbf{A}(\mathbf{r}_{\perp}, \xi; z) = (-\nabla_{\perp}^2 + \beta_2 \frac{\partial^2}{\partial \xi^2}) \mathbf{A}(\mathbf{r}_{\perp}, \xi; z) = H \mathbf{A}(\mathbf{r}_{\perp}, \xi; z). \quad (2)$$

Here, ξ is a (local time-like) space coordinate in the frame of the pulse, β_2 is the dimensionless GVD, $H = (-\nabla_{\perp}^2 + \beta_2 \partial^2/\partial \xi^2)$ is the spacetime propagator, and we separate z with a semicolon as it plays the role of a time-like running parameter.

Next, we assume a uniformly polarized beam $A(\mathbf{r}_{\perp}, \xi; z) \hat{\mathbf{e}}$, where $\hat{\mathbf{e}}$ is the complex polarization ($\hat{\mathbf{e}} = \hat{\mathbf{y}}$ as in our experiments [2], where there are no effects of spin angular momentum [10]), and find modal solutions to Eq. (2) for $\mathbf{r}_{\perp} = (x, y)$:

$$A_{mpq}(x, y, \xi; z) = A_{mpq}^{(0)} u_m(x; z) u_p(y; z) u_q^{\xi}(\xi; z) e^{ik_0 z}, \quad (3)$$

where

$$u_q^{\xi}(\xi; z) = \sqrt{\frac{w_{0\xi}}{w_{\xi}(z)}} H_q \left(\frac{\sqrt{2} \xi}{w_{\xi}(z)} \right) e^{-\xi^2/w_{\xi}^2(z)} e^{-ik_0 \xi^2/2\beta_2 R_{\xi}(z)} e^{i(q+1/2)\psi_{\xi}(z)}, \quad (4a)$$

$$u_m(x; z) = \sqrt{\frac{w_{0x}}{w_x(z)}} H_m \left(\frac{\sqrt{2} x}{w_x(z)} \right) e^{-x^2/w_x^2(z)} e^{ik_0 x^2/2R_x(z)} e^{-i(m+1/2)\psi_x(z)}. \quad (4b)$$

Here, H_m is a Hermite polynomial of order m , $w_x(z) = w_{0x}(1 + (z/z_{0x})^2)^{1/2}$, $R_x(z) = z(1 + (z_{0x}/z)^2)$, $\psi_x(z) = \tan^{-1}(z/z_{0x})$, and $z_{0x} = k_0 w_{0x}^2/2$ is the x -based Rayleigh range. The expression for $u_n(y)$ is identical to Eq. 4b with the substitution $x \rightarrow y$ everywhere. Associated with $u_q^{\xi}(\xi; z)$ we have $z_{0\xi} = k_0 w_{0\xi}^2/2|\beta_2|$, $w_{\xi}(z) = w_{0\xi}(1 + (z/z_{0\xi})^2)^{1/2}$, $R_{\xi}(z) = z(1 + (z_{0\xi}/z)^2)^{1/2}$, and $\psi_{\xi}(z) = \text{sgn}(\beta_2) \tan^{-1}(z/z_{0\xi})$. The quantities $w(z)$, $R(z)$ and $\psi(z)$ play the

role of z -variation in beam size, phase front curvature and Gouy phase shift as they do for standard transverse modes, except that here they also apply in the ξ domain.

The ‘‘spot sizes’’ w_{0x} , w_{0y} , and $w_{0\xi}$ describe the transverse space and temporal shape of the beam envelope of the lowest order mode ($(m, p, q) = (0, 0, 0)$) at $z = 0$, $A_{000}(x, y, \xi; z = 0) = A_{000}^{(0)} e^{-(x^2/w_{0x}^2 + y^2/w_{0y}^2)} e^{-\xi^2/w_{0\xi}^2} e^{-ik_0\xi}$, which approximates the input beam to our pulse shaper. The effective wavenumber k_0/β_2 associated with $u_q^\xi(\xi)$ accounts for the different rate of spreading in temporal dispersion compared to transverse beam diffraction. We have allowed our beam to have elliptical envelopes in both the $x - y$ (space) and $x - \xi$ (spacetime) planes, and different phase curvatures in x , y , and ξ . Our choice of HG basis functions for the solution of Eq. (2) is motivated by our experimental generation of STOV-carrying pulses using a $4f$ pulse shaper [2], which imposes rectilinearly-resolved ellipticity and astigmatism in both the space and spacetime domains.

We now consider propagation of the simplest STOV-carrying pulse generated by our pulse shaper, one with a spatiotemporal winding of topological charge $l = 1$ or $l = -1$. At $z = 0$, this pulse is constructed as

$$E(x, y, \xi; z = 0)_{(l=\pm 1)} = E_0 \left(\frac{\xi}{w_{0\xi}} \pm i \frac{x}{w_{0x}} \right) e^{-(x^2/w_{0x}^2 + y^2/w_{0y}^2)} e^{-\xi^2/w_{0\xi}^2}, \quad (5)$$

As we will see, the spacetime eccentricity ratio, $\alpha \equiv w_{0\xi}/w_{0x}$, is extremely important and will show up throughout these calculations. In the experiments, the y -direction is orthogonal to the pulse shaper grating rulings, and so after pulse reconstruction at the shaper output, the y -dependent envelope of the input pulse is reproduced [2].

In vacuum or in the very dilute medium (air) of the experiments [2], $\beta_2 = 0$ and $v_g = c$, and the dispersionless time-like mode factor (Eq. (4a)) becomes

$$u_q^\xi(\xi) = H_q \left(\frac{\sqrt{2}\xi}{w_{0\xi}} \right) e^{-\xi^2/w_{0\xi}^2}, \quad (6)$$

and Eq.(5) can be represented as linear combination of spacetime modes (Eqs. (4)) at $z = 0$:

$$E(x, y, \xi; z = 0)_{(l=\pm 1)} = E_0 u_0(y; 0) \left(u_0(x; 0) u_1^\xi(\xi; 0) \pm i u_1(x; 0) u_0^\xi(\xi; 0) \right). \quad (7)$$

Given this initial STOV field at $z = 0$, the propagator $H = (-\nabla_{\perp}^2 + \beta_2 \partial^2/\partial\xi^2)$ of Eq.(2) generates the full z -dependent evolution

$$E(x, y, \xi; z)_{(l=\pm 1)} = E_0 u_0(y; z) \left(u_0(x; z) u_1^\xi(\xi; z) \pm i u_1(x; z) u_0^\xi(\xi; z) \right) e^{ik_0z}, \quad (8)$$

For the case $w_{0x} = w_{0\xi}$ ($\alpha = 1$), the factor $u_1(x; z) u_0^\xi(\xi; z) \pm i u_0(x; z) u_1^\xi(\xi; z)$ is analogous to the superposition of the 0^{th} and 1^{st} order Hermite-Gaussian transverse modes to give the Laguerre-Gaussian spatial mode $LG_{0\pm 1}^{space} = u_0(x) u_1(y) \pm i u_1(x) u_0(y)$.

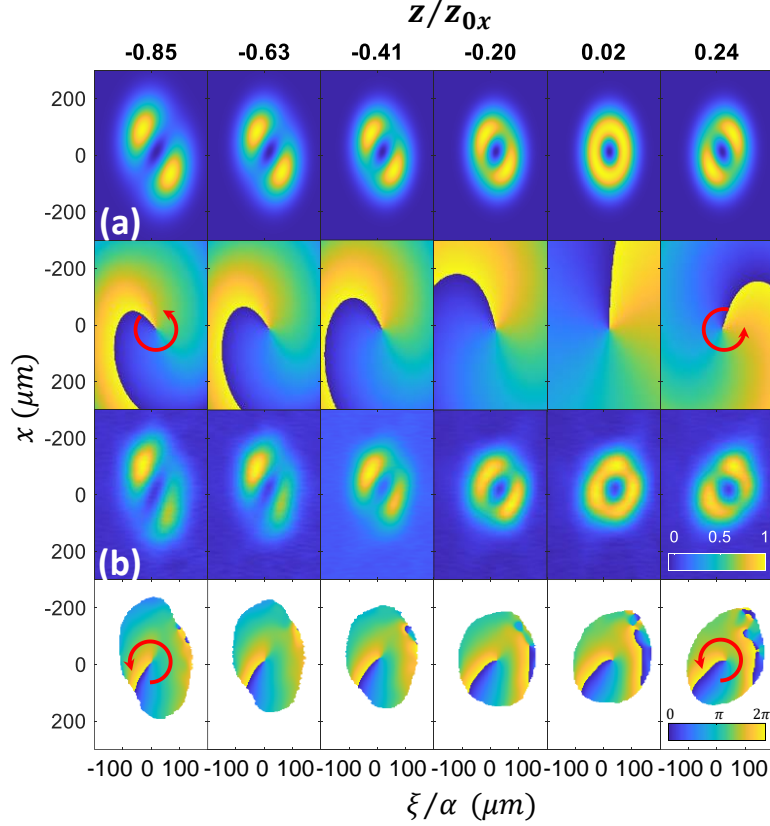


Figure 1. (a) Propagation evolution from $z/z_{0x} = -0.85$ to 0.24 of $E(x, y = 0, \xi; z)_{(l=+1)}$, an $l = +1$ STOV, simulated using the modal solution of Eq. (8). (a) Top row: Normalized intensity $|E(x, y = 0, \xi; z)_{(l=+1)}|^2$; Bottom row: Phase $\Phi(x, \xi) = \tan^{-1}[\text{Im}(\mathcal{E})/\text{Re}(\mathcal{E})]$ where $\mathcal{E} = e^{-ik_0z}E(x, y = 0, \xi; z)_{(l=+1)}$. The phase colourmap and red arrows show the direction of increasing phase. (b) Experiment: An $l = 1$ STOV is generated by passing a near-Gaussian pulse through a $4f$ pulse shaper with an $l = +1$ spiral phase plate at the shaper's Fourier plane (details in [2]), and the STOV amplitude and phase is captured in flight by TG-SSSI (details in [17]). The experimental Rayleigh length is $z_{0x} \approx 46\text{mm}$. The horizontal axis for both (a) and (b) is normalized to the experimental eccentricity $\alpha = w_{0\xi}/w_{0x} \sim 0.3$. The phase plots in (b) are blanked out in regions of low intensity, where phase extraction failed [11].

Figure 1 compares our theory and experiment, where Fig. 1(a) shows the amplitude and phase of $E(x, y = 0, \xi; z)_{(l=+1)}$ from $z = -0.85z_{0x}$ to $z = 0.24z_{0x}$, computed with Eq.(8). It is seen that the field is a donut at the beam waist ($z = 0$) (as constructed) and evolves into spatiotemporally offset lobes with opposite spacetime tilt on either side of $z = 0$, with transverse diffractive spreading widening the beam. Here, we have used $w_{0\xi}/w_{0x} = 0.3$ to match our experimental results, which are shown in Fig. 1(b). To capture the in-flight amplitude and phase profiles of these pulsed spatiotemporal structures, we have employed a new diagnostic, transient-grating single-shot supercontinuum spectral interferometry (TG-SSSI), which is fully described in [11]. The measurements are in excellent agreement with our mode-based calculation, capturing the STOV field's evolution from a donut into spatiotemporally offset lobes, and preserving the 2π phase winding [2].

For a more direct analysis of angular momentum of STOVs, we now express our HG-based mode solutions in spacetime polar coordinates (ρ, Φ) , where $x = \rho \sin\Phi$ and $\xi = \rho \cos\Phi$. In this description, we can describe the spacetime phase winding by the topological charge l and the single

function Φ , even for our general case of elliptical and astigmatic STOV pulses. The fundamental rectangular mode based on Eq. (3) is now written as

$$\begin{aligned} \mathcal{A}_{000}(\rho, y, \Phi; z) = & \mathcal{A}^{(0)} \sqrt{\frac{w_{0x}w_{0y}w_{0\xi}}{w_x(z)w_y(z)w_\xi(z)}} \exp\left(-\frac{\rho^2 \sin^2 \Phi}{w_x^2(z)} - \frac{y^2}{w_y^2(z)} - \frac{\rho^2 \cos^2 \Phi}{w_\xi^2(z)}\right) \\ & \times \exp\left[ik_0 \left(\frac{\rho^2 \sin^2 \Phi}{2R_x(z)} + \frac{y^2}{2R_y(z)} - \frac{\rho^2 \cos^2 \Phi}{2\beta_2 R_\xi(z)}\right)\right] \\ & \times \exp\left[\frac{-i}{2}(\psi_x(z) + \psi_y(z) - \psi_\xi(z))\right] \end{aligned} \quad (9)$$

and the $l = \pm 1$ STOV pulse from our pulse shaper is

$$\mathcal{E}(\rho, y, \Phi; z)_{(l=\pm 1)} = \mathcal{A}_{000}(\rho, y, \Phi; z) \left(\frac{\rho \cos \Phi}{w_\xi(z)} e^{i\psi_\xi(z)} \pm i \frac{\rho \sin \Phi}{w_x(z)} e^{-i\psi_x(z)} \right) e^{ik_0 z} \quad (10)$$

In our experiments, the y -dependent beam envelope shape, aside from transverse diffractive spreading, is preserved in propagation. So we henceforth neglect y variations in the beam by setting $y = 0$, noting that any 3D mode can be constructed by multiplying the (x, ξ) – dependent results by $u_n(y; z)$.

We now examine the STOV angular momentum, $\hat{y}L_y$, which is orthogonal to the $x - \xi$ plane of spatiotemporal phase circulation. First we must find the appropriate angular momentum operator L_y . To do so, we consider Eq. (2) along with the conservation of energy density flux [12], $\partial|\mathcal{E}|^2/\partial z = -\nabla \cdot \mathbf{j}$, where $\mathbf{j}_\perp = -i(2k_0)^{-1}(\mathcal{E}^* \nabla_\perp \mathcal{E} - \mathcal{E} \nabla_\perp \mathcal{E}^*)$ and $\mathbf{j}_\parallel = i\beta_2(2k_0)^{-1}[\mathcal{E}^*(\partial/\partial \xi)\mathcal{E} - \mathcal{E}(\partial/\partial \xi)\mathcal{E}^*]\hat{\xi}$. This gives $\mathbf{j} = k_0^{-1}|\mathcal{E}|^2(\nabla_\perp \Phi - \beta_2(\partial\Phi/\partial\xi)\hat{\xi}) = k_0^{-1}|\mathcal{E}|^2\nabla\Phi$, where $\nabla = \nabla_\perp - \hat{\xi}\beta_2(\partial/\partial\xi)$ is the spacetime gradient [1]. Therefore, the spacetime linear momentum operator is $\mathbf{p} = -i\nabla$, giving $L_y = (-i\mathbf{r} \times \nabla)_y = -i(\xi \partial/\partial x + x\beta_2 \partial/\partial \xi)$. In spacetime polar coordinates, this becomes

$$L_y = -i \left[\rho \sin \Phi \cos \Phi (1 + \beta_2) \frac{\partial}{\partial \rho} + (\cos^2 \Phi - \beta_2 \sin^2 \Phi) \frac{\partial}{\partial \Phi} \right] = L_y^e + L_y^i, \quad (11)$$

where we identify the first term as the extrinsic STOV angular momentum L_y^e , and the second term as the intrinsic STOV angular momentum L_y^i . Here, *intrinsic* refers to the origin-independent spatiotemporal angular momentum contribution, and *extrinsic* refers to the origin-dependent contribution which integrates to zero, $\langle L_y^e \rangle = 0$, when calculating the expectation value ($\langle \ \rangle$) of L_y by integrating over ρ ($0 \rightarrow \infty$) and Φ ($0 \rightarrow 2\pi$).

To calculate the STOV OAM associated with $\mathcal{E}(\rho, y, \Phi; z)_{(l=\pm 1)}$, we note that it is sufficient to do so at $z = 0$. This is because $\langle L_y^i \rangle$ is invariant with propagation, namely $(d/dz)\langle L_y \rangle = i(2k_0)^{-1}\langle [H, L_y] \rangle = 0$, owing to the fact that the propagation operator, $H = (-\nabla_\perp^2 + \beta_2 \partial^2/\partial \xi^2)$, and L_y commute: $[H, L_y] = 0$. This procedure greatly simplifies the calculation, especially for non-zero β_2 , where we consider the beam waist to be placed just inside

the material interface ($z = 0^+$) without additional chirp from the material yet induced. At $z = 0$, Eq. (10) becomes

$$\begin{aligned}\mathcal{E}_{STOV,\alpha}^{l=\pm 1} &= \mathcal{E}(\rho, y = 0, \Phi; z = 0)_{(l=\pm 1)} = \mathcal{A}_{000}(\rho, 0, \Phi; 0) \left(\frac{\rho \cos \Phi}{w_{0\xi}} \pm i \frac{\rho \sin \Phi}{w_{0x}} \right) e^{ik_0 z} \\ &= E_0 \frac{\rho}{w_{0\xi}} \exp \left(-\frac{\rho^2}{2w_{0\xi}^2} (\cos^2 \Phi + \alpha^2 \sin^2 \Phi) \right) \left(\frac{(1 \pm \alpha)}{2} e^{i\Phi} + \frac{(1 \mp \alpha)}{2} e^{-i\Phi} \right) e^{ik_0 z}\end{aligned}\quad (12)$$

This is nearly a linear combination of $LG_{0\pm 1}$ modes except for the Φ -dependent exponential prefactor, which loses its angle-dependence for $\alpha = 1$, yielding the symmetric spacetime Laguerre Gaussian mode $\mathcal{E}_{STOV,\alpha=1}^{l=\pm 1} = LG_{0\pm 1}^{spacetime} = E_0 (\rho/w_{0\xi}) \exp(-\rho^2/2w_{0\xi}^2) e^{\pm i\Phi}$

For arbitrary topological charge l , the l^{th} order STOV pulse is

$$\begin{aligned}\mathcal{E}_{STOV,\alpha}^l &= E_0 (\rho/w_{0\xi})^{|l|} \exp[-|l| (\rho^2/2w_{0\xi}^2) (\cos^2 \Phi + \alpha^2 \sin^2 \Phi)] (\cos \Phi \\ &\quad + i\alpha \operatorname{sgn}(l) \sin \Phi)^{|l|}.\end{aligned}\quad (13)$$

For a STOV with a phase winding of charge l and eccentricity $\alpha=1$, and for general α ,

$$\begin{aligned}\langle L_y \rangle_{l,\alpha=1} &= \langle \mathcal{E}_{STOV,\alpha=1}^l | L_y^i + L_y^e | \mathcal{E}_{STOV,\alpha=1}^l \rangle = \\ &\quad \langle \mathcal{E}_{STOV,\alpha=1}^l | L_y^i | \mathcal{E}_{STOV,\alpha=1}^l \rangle = \frac{1}{2} l (1 - \beta_2),\end{aligned}\quad (14a)$$

$$\langle L_y \rangle_{l,\alpha} = \langle \mathcal{E}_{STOV,\alpha}^l | L_y^i + L_y^e | \mathcal{E}_{STOV,\alpha}^l \rangle = \langle \mathcal{E}_{STOV,\alpha}^l | L_y^i | \mathcal{E}_{STOV,\alpha}^l \rangle = \frac{1}{2} l (\alpha - \beta_2/\alpha), \quad (14b)$$

where $\langle L_y^e \rangle = 0$, and where $\langle L_y \rangle$ depends explicitly on topological charge l , STOV eccentricity α and material dispersion β_2 .

This is a remarkable result, for which we will first consider the case $\alpha = 1$, a space-time symmetric STOV. As seen in the earlier expression for $\mathcal{E}_{STOV,\alpha=1}^{l=\pm 1}$, this is analogous to the symmetric vortex characteristic of a stigmatic Laguerre Gaussian mode. For the case of vacuum ($\beta_2 = 0$), $\langle L_y \rangle = l/2$: STOV OAM is *quantized in half integer units*. Furthermore, it shows that in dispersive media, a quantum interpretation of the role of β_2 is strongly suggested, where one might consider the material disturbance induced by a STOV-encoded photon field as a new type of quasiparticle, a ‘‘STOV polariton’’.

An explanation for half-integral STOV orbital angular momentum in vacuum is that electromagnetic energy density flow in the pulse frame is purely along $\pm x$, or along ∇_{\perp} . For $l = +1$, energy density flows along $+x$ in advance of the STOV singularity and along $-x$ behind it, as seen in experiments and simulations [2]. Because $\beta_2 = 0$ in vacuum or extremely dilute media, there is no energy flow along ξ . This is in contrast to a standard $LG_{0\pm 1}$ mode, where electromagnetic energy circulates clockwise or counterclockwise around the singularity. While the algebra of angular momentum operators places no prohibition on half integral angular momenta, it is the demand for single-valuedness of spatial wavefunctions over a 2π coordinate rotation that gives rise to integer OAM. However, single valuedness is apparently not a requirement for these spatiotemporal rotations.

To address this situation in quantum terms, we consider a two-step spacetime rotation $(\rho, \Phi) \rightarrow (\rho, \Phi + \Delta\Phi) \rightarrow (\rho, \Phi)$ generated by successive applications of the rotation operator $\mathbb{R}(\Delta\Phi) = \exp(-i\Delta\Phi L_y^i)$ to a spacetime-dependent wavefunction $\psi(\rho, \Phi)$. The composite operator is $\mathbb{R}(-\Delta\Phi)\mathbb{R}(\Delta\Phi) = \exp(i\Delta\Phi L_y^i) \exp(-i\Delta\Phi L_y^i)$, where we consider the vacuum case ($\beta_2 = 0$) with $L_y^i = -i \cos^2 \Phi \partial / \partial \Phi$. For ease of calculation, we assume a small rotation $|\Delta\Phi| \ll 1$ so that $\mathbb{R}(-\Delta\Phi)\mathbb{R}(\Delta\Phi) = 1 + (\Delta\Phi)^2 \cos^2 \Phi [-\sin 2\Phi \partial / \partial \Phi + \cos^2 \Phi \partial^2 / \partial \Phi^2] + \dots$, deviating from unity and indicating that \mathbb{R} is not invertible in vacuum. This suggests that a spacetime swap of 2 identical photons around the singularity from (ρ, Φ) to $(\rho, \Phi \pm \Delta\Phi)$ in a STOV quantum wavepacket state would not leave the state phase invariant, unlike a swap in purely space coordinates.

By contrast, a composite rotation $(r, \varphi) \rightarrow (r, \varphi + \Delta\varphi) \rightarrow (r, \varphi)$ in 3D space coordinates generated by, say, the z-component of angular momentum $L_z = -i \partial / \partial \varphi$ gives $\mathcal{R}(-\Delta\varphi)\mathcal{R}(\Delta\varphi) = 1$ for any finite $\Delta\varphi$. This leads to the demand for single-valuedness of the space-only wavefunction $\psi_{space}(r, \varphi)$ and integral OAM. However, integral STOV OAM is also possible: inspection of Eq. (11) shows that for $\beta_2 = -1$, $L_y^i = -i \partial / \partial \Phi$ and rotations are invertible, leading to integral STOV OAM as discussed later.

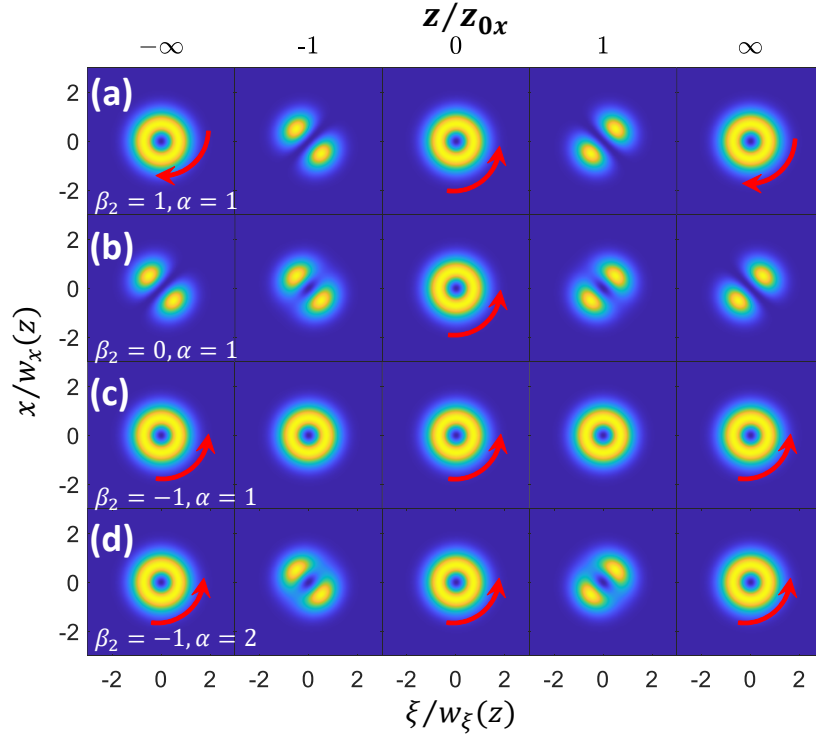


Figure 2. Plots of $|E(x, y = 0, \xi; z)_{(l=+1)}|^2$, computed using Eq. (8), of propagation of $l = 1$, $\alpha = w_{0\xi}/w_{0x}$ STOVs in vacuum and in a dispersive medium with normalized GVD β_2 . Propagation is through the beam waist ($z/z_{0x} = 0$) and into the far field ($\pm\infty$). The red arrows indicate the direction of spatiotemporal phase gradient $\nabla\Phi(x, \xi)$. Row **(a)**: $\beta_2 = 1$ (normal dispersion), $\alpha = 1$ (symmetric STOV). While $\langle L_y \rangle = 0$ (see Eq. (14)), $\nabla\Phi(x, \xi)$ flips direction. Row **(b)**: $\beta_2 = 0$ (vacuum), $\alpha = 1$ (symmetric STOV). Here, similar to Fig. 1, the intensity evolves to spatiotemporally offset lobes of opposite tilt in the $-\infty$ and $+\infty$ far fields, with $\nabla\Phi(x, \xi)$ maintaining direction. Row **(c)**: $\beta_2 = -1$ (anomalous dispersion), $\alpha = 1$ (symmetric STOV). Here, $\langle L_y \rangle = 1$, and the mode shape and $\nabla\Phi(x, \xi)$ are self-similarly preserved throughout propagation, resembling a pure free space mode. Row **(d)**: $\beta_2 = -1$ (anomalous dispersion), $\alpha = 2$ (asymmetric STOV). Here, the near and far field mode shapes coincide, with the direction of $\nabla\Phi(x, \xi)$ preserved throughout propagation.

We now examine the physical meanings of β_2 and α in Eqs. (14). For simplicity, we first consider $\alpha = 1$ and later return to the interpretation of α . Note that in Eq. (13) we used the vacuum STOV ($\beta_2 = 0$) –with its original spectral phase– implicitly at $z = 0^+$ (just inside the material) to calculate $\langle L_y \rangle_l$. But in reality, even at $z = 0^+$, the STOV spectral phase would have been modified by the dispersive material. Therefore, the added term $-(l/2)\beta_2$ in $\langle L_y \rangle_l$, which is imposed by the full β_2 -dependent L_y^l operator (Eq. (11)), represents sharing of the pulse OAM with the material *for a given phase winding l* . This suggests that the material has an electromagnetic OAM response quantized in half integer steps of β_2 –we identify this object as a bulk medium “STOV polariton”. For the case $\beta_2 = 1$, $\langle L_y \rangle_l = 0$ and the medium has apparently taken up $l/2$ units of angular momentum from the STOV field. It is interesting to note that $\beta_2 = 1$ for materials with a quadratic dispersion relation ($\omega \propto k^2$) or ‘effective mass’ for photons. This is a known dispersion dependence for polaritons [13, 14]. For an anomalously dispersive material with $\beta_2 = -1$, we get $\langle L_y \rangle_l = l$, which we interpret either that the STOV OAM is split between the photon and polariton field, or that the self-consistent electromagnetic object in the dispersive material has integral spatiotemporal OAM. Other values of β_2 give a range of OAM contributions between photons and polaritons.

We now address the physical meaning of α . As clearly pointed out in detail by Plick *et al.* [15] in the context of spatial OAM, there is nothing sacrosanct about circular symmetry. Spatial LG modes with circular symmetry are easily generated in the lab, as are HG modes [7], and as solutions to the paraxial wave equation (PWE), both types of functions form complete basis sets. It is with LG modes, however, that the OAM coincides with the topological charge l of the vortex, while for HG modes, two quantum numbers are needed to describe OAM. Plick *et al.* [15] show that the intrinsic OAM of ‘elliptical’ monochromatic beams (beams with $w_{0x} \neq w_{0y}$ but common curvature and Gouy phase) is determined by the ratio w_{0y}/w_{0x} *on a per-photon basis*. That is, the transverse beam shape is encoded onto the photon OAM, albeit with OAM in integer steps as appropriate for 3D space. Although our spacetime paraxial wave equation (Eq. (2)) is different than the spatial PWE, the conclusions regarding the STOV eccentricity parameter $\alpha = w_{0\xi}/w_{0x}$ are exactly the same: α is encoded onto the intrinsic STOV OAM of photons. In vacuum, STOV OAM is quantized in half-integral steps of α , while in a dispersive medium, it is quantized in half integral steps of $(\alpha - \beta_2/\alpha)$.

Considering the limit $\alpha \rightarrow 0$ in vacuum (and ignoring the breakdown in the slowly varying envelope approximation used to obtain Eq. (2)), $\langle L_y \rangle_l \rightarrow 0$ as is appropriate: the pulse loses the time-like contribution to its vorticity. In a dispersive medium, $\alpha \rightarrow 0$ corresponds to a shrinking of temporal pulsewidth accompanied by increasing bandwidth, for which dispersion and the phase gradient contribution of $\hat{\xi}\beta_2\partial\Phi/\partial\xi$ to $\langle L_y \rangle_l$ increase significantly. In classical terms, electromagnetic energy flow in $\hat{\xi}$ dominates that in \hat{x} . To be consistent with the *given* topological charge l , $|\langle L_y \rangle_l|$ must become large. For $\alpha \rightarrow \infty$, the pulse becomes very long and the effect of dispersion goes away ($\beta_2/\alpha \rightarrow 0$). Then, to be consistent for a given l , the phase gradient $\hat{x}\partial\Phi/\partial x$ must become very large, as does $\langle L_y \rangle_l$. In general, heuristic electromagnetic energy flow arguments like these provide good physical insight into the effects of varying α and β_2 .

Figure 2 shows plots of $|E(x, y = 0, \xi; z)_{(l=+1)}|^2$, computed using the modal solution of Eq. (8), of propagation of $l = 1$, $\alpha = w_{0\xi}/w_{0x}$ STOVs in vacuum and in a dispersive medium characterized by β_2 . A range of interesting behaviour is observed as discussed in the figure caption, but the main points are as follows: (1) in dispersive materials, the phase winding direction can flip

to maintain OAM conservation, and one cannot predict spatiotemporal phase gradients purely based on the topological charge l ; (2) A donut-shaped STOV launched in vacuum or dilute media in general does not stay together as a donut; the spatio-temporal energy flow, via the term \mathbf{j}_\perp (see discussion near Eq. 11) forces the donut into spatiotemporally offset lobes, as also seen in Fig. 1 and Ref [2]; (3) There exists a self-similar STOV mode with *integral* OAM for $\alpha = 1$ and $\beta_2 = -1$ (Fig. 2(c)) of bosonic character. Classically, this is visualized as balanced STOV energy flow along $\hat{\mathbf{x}}$ and $\hat{\mathbf{\xi}}$.

In summary, we have presented a new class of light states with half-integral orbital angular momentum orthogonal to propagation. In vacuum, they are quantized in half integer units of α , the STOV eccentricity parameter. In a dispersive medium, they are quantized in half integer units of $(\alpha - \beta_2/\alpha)$, where β_2 is the normalized group velocity dispersion of the material, where we consider this OAM as shared between a photon and a STOV polariton, or as the OAM of the self-consistent field in the material. We expect that our results will motivate further studies into the physics and applications of STOVs.

Acknowledgements. The authors thank Nihal Jhajj, who began this work, and Steve Rolston, for useful discussions. This work is supported by the Air Force Office of Scientific Research (FA9550-16-1-0121, FA9550-16-1-0284), the Office of Naval Research (N00014-17-1-2705, N00014-20-1-2233), and the National Science Foundation (PHY2010511).

References

- [1] N. Jhajj, I. Larkin, E. W. Rosenthal, S. Zahedpour, J. K. Wahlstrand, and H. M. Milchberg, "Spatiotemporal Optical Vortices," *Phys. Rev. X* **6**, 031037 (2016).
- [2] S. W. Hancock, S. Zahedpour, A. Goffin, and H. M. Milchberg, "Free-space propagation of spatiotemporal optical vortices," *Optica* **6**, 1547 (2019).
- [3] A. Chong, C. Wan, J. Chen, and Q. Zhan, "Generation of spatiotemporal optical vortices with controllable transverse orbital angular momentum," *Nat. Photonics* **14**, 350 (2020).
- [4] S. W. Hancock, S. Zahedpour, and H. M. Milchberg, "Orbital angular momentum conservation in second-harmonic generation with spatiotemporal optical vortices," in *Frontiers in Optics + Laser Science APS/DLS, OSA Technical Digest (Optical Society of America, 2020)*, paper FM7C.6.
- [5] S. W. Hancock, S. Zahedpour, and H. M. Milchberg, "Second-Harmonic Generation of Spatiotemporal Optical Vortices," in *High-Brightness Sources and Light-Driven Interactions Congress, OSA Technical Digest (Optical Society of America, 2020)*, paper JM3A.21.
- [6] S. W. Hancock, S. Zahedpour, and H. M. Milchberg, "Second harmonic generation of spatiotemporal optical vortices (STOVs) and conservation of orbital angular momentum," submitted for publication, <https://arxiv.org/abs/2012.10806>
- [7] L. Allen, M. W. Beijersbergen, R. J. C. Spreeuw, and J. P. Woerdman, "Orbital angular momentum of light and the transformation of Laguerre-Gaussian laser modes," *Phys. Rev. A* **45**, 8185 (1992).]
- [8] A. P. Sukhorukov and V. V. Yangirova, in edited by M. A. Karpierz, A. D. Boardman, and G. I. Stegeman (*International Society for Optics and Photonics, 2005*).
- [9] K. Y. Bliokh and F. Nori, *Phys. Rev. A* **86**, 033824 (2012).
- [10] K. Bliokh, "Spatiotemporal Vortex Pulses: Angular Momenta and Spin-Orbit Interaction," <https://arxiv.org/abs/2102.02180>

- [11] S.W. Hancock, S. Zahedpour, and H. Milchberg, "Transient-grating single-shot supercontinuum spectral interferometry (TG-SSSI)," *Opt. Lett.* **46**, 1013 (2021).
- [12] A. Lotti, A. Couairon, D. Faccio, and P. Di Trapani, "Energy-flux characterization of conical and space-time coupled wave packets," *Phys. Rev. A* **81**, 023810 (2010)
- [13] C.F. Klingshirn, *Semiconductor Optics*, Springer (2012).
- [14] M. J. Gullans, J. D. Thompson, Y. Wang, Q.-Y. Liang, V. Vuletić, M. D. Lukin, and A. V. Gorshkov, "Effective Field Theory for Rydberg Polaritons," *Phys. Rev. Lett.* **117**, 113601 (2016)
- [15] W. N. Plick, M. Krenn, R. Fickler, S. Ramelow, and A. Zeilinger, "Quantum orbital angular momentum of elliptically symmetric light," *Phys. Rev. A* **87**, 033806 (2013).